Light-activated protein-conjugation and 89Zr-radiolabelling with water-soluble desferrioxamine derivatives

Guillou, Amaury ; Earley, Daniel ; Holland, Jason Philip

Abstract: Protein-conjugates are vital tools in biomedical research, drug discovery and imaging science. For example, functionalised monoclonal antibodies (mAbs) coupled to the desferrioxamine B (DFO) chelate and radiolabelled with 89Zr are used as radiopharmaceuticals for diagnostic positron emission tomography (PET). In this context, protein functionalisation requires the formation of a covalent bond which must be achieved without compromising the biological properties of the mAb. Photochemistry offers new synthetic routes toward protein-conjugates like 89Zr-mAbs but to harness the potential of light-induced conjugation reactions new photoactivatable reagents are required. Here, we introduce two photoactivatable DFO-derivatives functionalised with an aryl azide (ArN3) for use in light-activated conjugation and radiosynthesis of 89Zr-mAbs. Incorporation of a tris-polyethylene glycol (PEG)3 linker between DFO and the ArN3 group furnished water-soluble chelates that were used in the one-pot, photoradiosynthesis of different 89Zr-radiolabelled protein-conjugates with radiochemical yields up to 72.9±1.9%. Notably, the DFO-PEG3 chelates can be readily synthesised in accordance with Good Laboratory Practice (GLP), which will facilitate clinical trials with photoradiolabelled 89Zr-mAbs.

DOI: https://doi.org/10.1002/chem.202001755

Chemistry
A European
Journal

Chemistry Europe
European Chemical Societies Publishing

Accepted Article

Title: Light-activated protein-conjugation and 89Zr-radiolabelling with water-soluble desferrioxamine derivatives

Authors: Amaury Guillou, Daniel Earley, and Jason P. Holland

To be cited as: *Chem. Eur. J.* 10.1002/chem.202001755

Link to VoR: https://doi.org/10.1002/chem.202001755

WILEY-VCH

10.1002/chem.202001755

WILEY-VCH

COMMUNICATION

Light-activated protein-conjugation and ^{89}Zr-radiolabelling with water-soluble desferrioxamine derivatives

Amaury Guillou,[a] Daniel F. Earley[a] and Jason P. Holland*[a]

Abstract: Protein-conjugates are vital tools in biomedical research, drug discovery and imaging science. For example, functionalised monoclonal antibodies (mAbs) coupled to the desferrioxamine B (DFO) chelate and radiolabelled with ^{89}Zr are used as radiopharmaceuticals for diagnostic positron emission tomography (PET). In this context, protein functionalisation requires the formation of a covalent bond which must be achieved without compromising the biological properties of the mAb. Photochemistry offers new synthetic routes toward protein-conjugates like ^{89}Zr-mAbs but to harness the potential of light-induced conjugation reactions new photoactivatable reagents are required. Here, we introduce two photoactivatable DFO-derivatives functionalised with an aryl azide (ArN_3) for use in light-activated conjugation and radiosynthesis of ^{89}Zr-mAbs. Incorporation of a *tris*-polyethylene glycol $(PEG)_3$ linker between DFO and the ArN_3 group furnished water-soluble chelates that were used in the one-pot, photoradiosynthesis of different ^{89}Zr-radiolabelled protein-conjugates with radiochemical yields up to 72.9±1.9%. Notably, the DFO-PEG_3 chelates can be readily synthesised in accordance with Good Laboratory Practice (GLP), which will facilitate clinical trials with photoradiolabelled ^{89}Zr-mAbs.

Reagents that undergo photochemical activation are striking alternatives to the well-established thermochemically activated routes toward protein functionalisation.[1,2] The absorption of light by compounds containing benzophenone, diazirine or ArN_3 groups generates highly reactive diradical, carbene or nitrene intermediates, which under optimised conditions can form covalent bonds to protein. In a biologically compatible medium, these reactive intermediates exhibit lifetimes in the nanosecond (ns) to microsecond (μs) range. Such extreme reactivity is inaccessible from traditional thermochemically-mediated processes and mechanistically implies that if successful *bimolecular* protein-conjugation is to be achieved, the coupling step must kinetically outcompete other non-productive background reactions including hydrolysis, protonation or quenching by oxygen.[3–5]

We recently demonstrated that metal ion binding chelates functionalised with a photoactivatable ArN_3 group can be used to prepare radiolabelled antibodies by either a two-step conjugation and radiolabelling process or by a novel one-pot approach.[6–11] Simultaneous ^{89}Zr-radiolabelling and light-induced conjugation using a photoactivatable DFO-ArN_3 derivative produced viable PET radiotracers (Scheme 1).[7,11] Additionally, the photochemical conjugation process is compatible with standard formulation buffers, which allows direct synthesis of radiolabelled-mAbs from approved drugs like Herceptin™. Experimentally, the efficiency and reproducibility of the photochemistry depends on several factors including the reaction geometry, light intensity, emission wavelength, and the stability and solubility of the reagents in basic conditions.

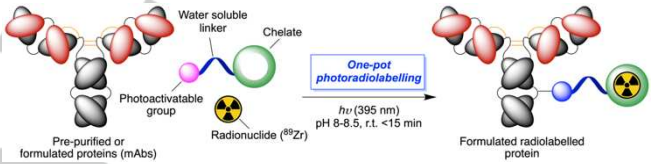

Scheme 1. *Illustration of the general concept of the one-pot, light-activated photoradiolabelling to produce ^{89}Zr-mAbs.*

There have been many reports of alternative, octadentate chelates for selective radiolabelling of proteins with $^{89}Zr^{4+}$ ions.[12,13] In the clinic, DFO remains the chelate of choice for PET imaging with ^{89}Zr-mAbs. DFO is normally conjugated to mAbs *via* reactive groups such as activated esters or benzyl-isothiocyanates that are introduced to the terminal primary amine of the chelate. A limitation is that functionalisation of the primary amine of DFO often compromises the water-solubility, and can lead to problems controlling the conjugation chemistry.

Two approaches to circumvent solubility issues have been reported. Richardson-Sanchez *et al*. hijacked the biosynthetic machinery of *Streptomyces pilosus* to install ether groups into the backbone of the hexadentate DFO ligand, bioisosterically replacing the $–(CH_2)_5–$ unit with a $–(CH_2)_2O(CH_2)_2–$ moiety to give the water-soluble DFO-O_3 ligand (Figure 1).[14] Similar methods were also used to introduce redox-active disulfide bonds.[15] In parallel, Briand *et al*. used solid-phase synthesis to produce the water-soluble, octadentate chelate oxoDFO* which incorporated four ether groups in the ligand backbone.[16] Computational studies revealed that the ether functionalities in DFO-O_3 and oxoDFO* could potentially increase the thermodynamic stability of $^{89}Zr^{4+}$ complexes by reducing ligand strain.[17] Although biosynthetic chemistry and solid-phase techniques are advanced routes to new chelates, and solubility characteristics were improved, these chemistries present challenges for making GLP-compliant materials for use in clinical translation. Here, we report a simple approach to the synthesis of water-soluble DFO derivatives coupled to a photoactivatable ArN_3 group *via* a polyethylene glycol $(PEG)_3$ linker.

[a] Dr A. Guillou, Dr D. F. Earley, Prof. Dr J. P. Holland*
University of Zurich, Department of Chemistry, Winterthurerstrasse 190, Zurich, CH-8057, Switzerland
E-mail: jason.holland@chem.uzh.ch
Tel: +41.44.63.53.990
Homepage: http://www.hollandlab.org

Supporting information for this article is given *via* a link at the end of the document.

10.1002/chem.202001755

COMMUNICATION

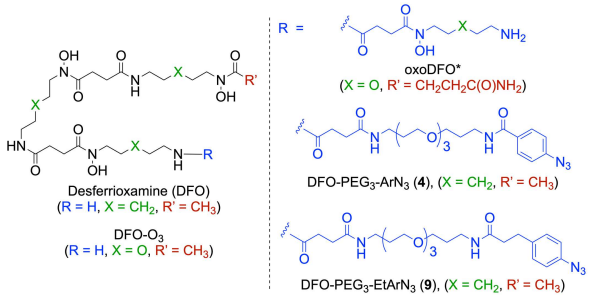

Figure 1. *Chemical structures of DFO and four water-soluble DFO-derivatives. Compounds* ***4*** *and* ***9*** *are reported in this work.*

The functionalised DFO-PEG$_3$-ArN$_3$ (**4**; Scheme 2) and DFO-PEG$_3$-EtArN$_3$ (**9**; supporting Scheme S1) metal binding chelates were synthesised by using standard chemical transformations with overall yields of 36% and 14%, respectively. Full experimental details and characterisation data, including ^{1}H and ^{13}C{^{1}H} NMR spectroscopy and high-resolution electrospray ionisation mass spectrometry for compounds **1** to **9**, are provided in the supporting information (Figures S1–S37). The synthesis of compound **4** was achieved on a gram scale with simple isolation by reversed-phase C18 flash chromatography.

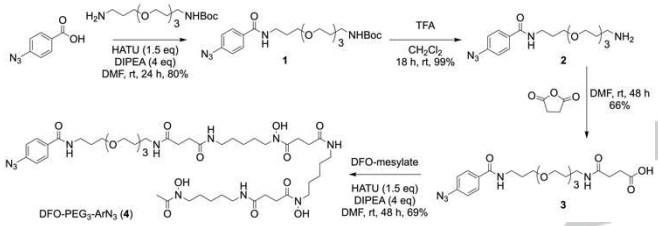

Scheme 2. *Multi-step synthesis of the water-soluble, photoactivatable chelate, DFO-PEG$_3$-ArN$_3$ (**4**).*

^{89}Zr-radiolabelling reactions were performed at room temperature by adding aliquots of [^{89}Zr][Zr(C$_2$O$_4$)$_4$]$^{4-}$ (^{89}Zr-oxalate) to samples of compounds **4** or **9** dissolved in water and adjusting to pH8.0–8.5 with Na$_2$CO$_3$ (the optimum range for our photoradiosynthesis).[6,7] ^{89}Zr-radiolabelling was characterised by using radio-instant thin layer chromatography (radio-ITLC) and radio-HPLC methods (Figure 2). Quantitative ^{89}Zr-radiolabelling yields were obtained in <5 min. The chemical identity and radiochemical purity (RCP) of the products were confirmed by comparison of the HPLC elution profiles to that of the corresponding non-radioactive ^{nat}Zr-complexes (Figure 2B; blue and green traces; Figure S37 for $^{nat/89}$Zr-**9**$^+$ data). Irradiation of the [^{89}Zr]ZrDFO-PEG$_3$-ArN$_3$ ($^{nat/89}$Zr-**4**$^+$) samples with a powerful light-emitting diode (LED) with peak emission at 395 nm confirmed the photochemical activity of the complex (Figure 2B, red trace). Complete photoactivation of $^{nat/89}$Zr-**4**$^+$ was observed in <15 min.

Next, we evaluated the efficiency of compounds **4** and **9** in the photoradiosynthesis of a series of ^{89}Zr-radiolabelled proteins. Formulated protein substrates included human serum albumin (HSA), the engineered antibody onartuzumab (formulated as MetMAb^{TM}), and the humanised IgG$_1$ immunoglobulin trastuzumab (formulated as Herceptin^{TM}). Simultaneous (one-pot) photoradiolabelling reactions were performed in accordance with Scheme 3.[7,11]

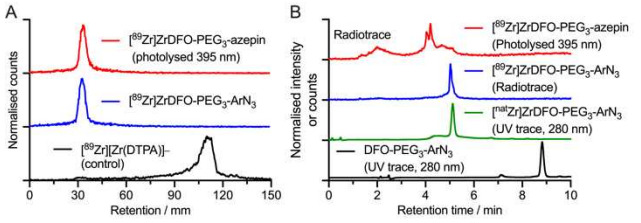

Figure 2. *Radioactive chromatography showing: (A) radio-ITLC chromatograms of [^{89}Zr]ZrDFO-PEG$_3$-ArN$_3$ before (blue) and after (red) photolysis at 395 nm. The elution profile of [^{89}Zr][Zr(DTPA)]$^-$ (black) is shown as a control. (B) HPLC chromatograms shown the elution profile of compound **4** (black trace), the nonradioactive ^{nat}Zr-complex (green), and the [^{89}Zr]ZrDFO-PEG$_3$-ArN$_3$ before (blue) and after (red) photolysis at 395 nm.*

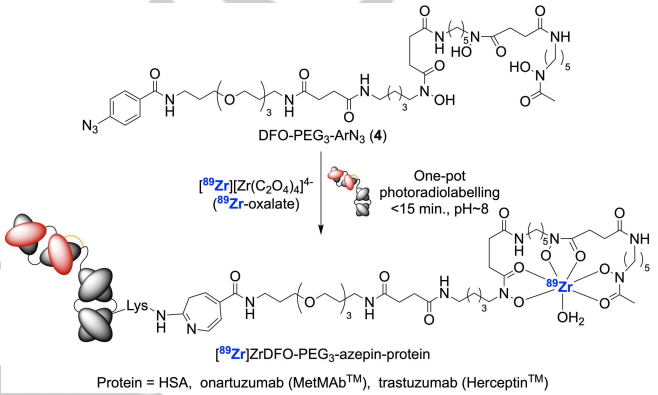

Scheme 3. *Simultaneous (one-pot) protein conjugation and ^{89}Zr-radiolabelling of proteins using light-induced activation of DFO-PEG$_3$-ArN$_3$ (**4**). Successful protein radiolabelling was achieved with HSA (MW = 69.08 kDa), onartuzumab (99.16 kDa) and trastuzumab (MW ~150 kDa).*

Aliquots of the photoactivatable compounds **4** or **9** were mixed with the separate protein solutions in transparent glass vials, and then [^{89}Zr][Zr(C$_2$O$_4$)$_4$]$^{4-}$ was added to give final reaction volume of 150 μL. Reaction mixtures were stirred gently and irradiated (395 nm) for 15 min. at room temperature to ensure complete photoactivation. Aliquots of the crude reaction mixtures were retained for analysis and fractions were purified by preparative size-exclusion gel filtration (PD-10) methods. Crude and purified samples were analysed by radio-ITLC, analytical PD-10 size-exclusion chromatography (SEC), and automated HPLC coupled to a SEC gel-filtration column (Figure 3 and supporting Figures S38–S41).

After irradiation, isolated and decay-corrected (d.c.) radiochemical yields (RCYs) for the [^{89}Zr]ZrDFO-PEG$_3$-azepin-protein reactions with compound **4** were 72.9±1.9% for HSA, 64.5±6.7% for MetMAb^{TM}, and 58.3±3.4% for Herceptin^{TM} (n = 3 independent measurements for each reaction; with final protein concentrations in the reaction mixtures of 175 μM, 141 μM, 77 μM, respectively). For comparison, reactions to form [^{89}Zr]ZrDFO-PEG$_3$-azepin-HSA by irradiation at a shorter wavelength (365 nm) gave an average RCY of 70.7±2.3% (n = 3). For each reaction the radiochemical purity (RCP) of the isolated products was >90% (determined by HPLC). Protein aggregation was <5%, and when compared to the analysis of the protein stock solutions, did not increase after irradiation. The equivalent ^{89}Zr-radiolabelling HSA

10.1002/chem.202001755

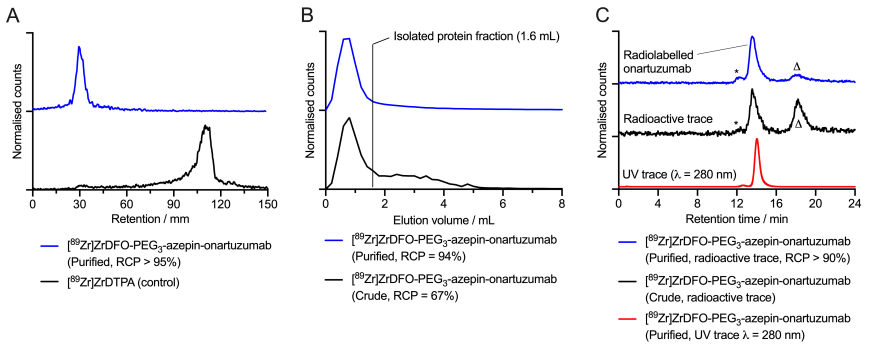

Figure 3. *Radioactive chromatography showing: (A) radio-ITLC chromatograms of purified (blue) [^{89}Zr]ZrDFO-PEG$_3$-azepin-onartuzumab (MetMAb^{TM}). (B) Analytical SEC (PD-10) elution profiles showing the crude (black) and purified (blue) samples of [^{89}Zr]ZrDFO-PEG$_3$-azepin-onartuzumab. (C) Radioactive and electronic absorption HPLC chromatograms acquired using SEC gel-filtration showing analysis of the crude (black) and purified (blue) samples. Note (*) corresponds to a protein aggregate fraction; (Δ) corresponds to the photolysed [^{89}Zr]ZrDFO-PEG$_3$-ArN$_3$ byproducts.*

with compound **9** to form [^{89}Zr]ZrDFO-PEG$_3$-Et-azepin-HSA was also performed and gave an isolated d.c. RCY of 59.6±3.6% (n = 3). Although both compounds **4** and **9** are water-soluble, the dissolution of compound **9** in water was improved by adding <1% DMSO/H_2O. The addition of DMSO does not appear to interfere with the photoactivation or protein-conjugation steps. In contrast to our previous work with DFO-ArN$_3$, the facile reactions and high reproducibility of these experiments likely stems from the enhanced water-solubility of compounds **4** and **9**.[7]

The slightly improved solubility profile of compound **4** compared with compound **9** (which contains a more lipophilic ethylene group) led us to pursue further biological studies using [^{89}Zr]ZrDFO-PEG$_3$-azepin-onartuzumab. Chelate challenge experiments demonstrated that [^{89}Zr]ZrDFO-PEG$_3$-azepin-onartuzumab remained stable with respect to changes in RCP during incubation with excess diethylenetriamine pentaacetate (DTPA; >50 mM, pH7, 37 °C, 94 h; supporting Figure S42). After incubation for 4 days, <16% of the radioactivity was found to transchelate to DTPA to give [^{89}Zr][Zr(DTPA)]$^-$ which is consistent with the excellent stability of the ZrDFO complex under physiological conditions.[18] Saturation binding experiments were also performed by incubating [^{89}Zr]ZrDFO-PEG$_3$-azepin-onartuzumab with human gastric carcinoma MKN-45 cells (supporting Figure S43). These cellular studies revealed that [^{89}Zr]ZrDFO-PEG$_3$-azepin-onartuzumab was immunoreactive and displayed specific binding to the human hepatocyte growth-factor receptor (c-MET).[19]

Encouraged by the experimental results *in vitro*, we pursued small-animal PET imaging and biodistribution experiments in female athymic nude mice bearing subcutaneous MKN-45 human xenografts on the right shoulder (Figure 4; maximum intensity project [MIP] images are given in supporting Figure S44). The photoradiosynthesis of [^{89}Zr]ZrDFO-PEG$_3$-azepin-onartuzumab was scaled up and the isolated product was formulated in sterile PBS (pH7.4). Two groups of animals (n = 5 mice/group) received between 0.46–0.60 MBq of ^{89}Zr radioactivity. The first group received a normal dose containing a total mass of 59–72 μg of onartuzumab per animal while the same activity dose but an increased protein mass (823–834 μg of onartuzumab per animal) were administered to the control (blocking) group to modulate the tumour uptake by saturating the available c-MET receptors. Quantitative volume-of-interest (VOI) analysis from the PET images revealed high accumulation of ^{89}Zr-radioactivity in the tumours of the normal group reaching 14.3±1.7 %ID cm^{-3} (n = 5) by 72 h post-administration (supporting Figure S45). In comparison, radiotracer uptake in tumours of the blocking group showed a statistically significant decrease of over 40% and reached only 8.5±0.9 %ID cm^{-3} (n = 5) after 72 h (Student's t-test P-value < 0.001). These data confirmed that [^{89}Zr]ZrDFO-PEG$_3$-azepin-onartuzumab remained immunoreactive and displayed specific binding to the c-MET receptor *in vivo*.

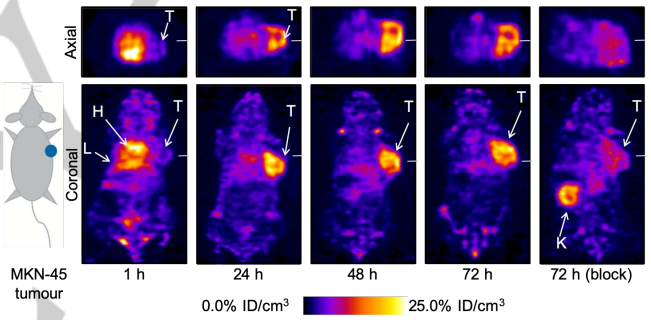

Figure 4. *Coronal and axial PET images taken through the centre of the tumours showing the spatial distribution of [^{89}Zr]ZrDFO-PEG$_3$-azepin-onartuzumab over time after intravenous administration in mice bearing MKN-45 tumours. T = tumour, H = heart, L = liver, K = kidney.*

As additional controls, PET images were also recorded at multiple time points (0 – 16 h post-administration) in mice that received [^{89}Zr]ZrDFO-PEG$_3$-ArN$_3$ (Figure S46; synthesised in the dark) or a photolysed sample of [^{89}Zr]ZrDFO-PEG$_3$-azepin that was irradiated at 395 nm for 15 min. at room temperature in the absence of protein (Figure S47). VOI analysis (supporting Figure S48 and Table S1) revealed that [^{89}Zr]ZrDFO-PEG$_3$-ArN$_3$ or the photolysed byproducts have dramatically different pharmacokinetic profiles when compared with [^{89}Zr]ZrDFO-PEG$_3$-azepin-onartuzumab. [^{89}Zr]ZrDFO-PEG$_3$-ArN$_3$ and photolysed [^{89}Zr]ZrDFO-PEG$_3$-azepin were cleared rapidly from the circulation as demonstrated by the absence of ^{89}Zr-activity in the heart/blood pool. Both samples showed unusually high uptake in the gall bladder with rapid elimination of ^{89}Zr-activity observed *via* both intestinal and renal pathways. By 2 h post-administration, ^{89}Zr-activity in the bladder and kidneys was almost entirely cleared whereas activity in the abdominal region migrated from the small to the large intestine. These PET data indicate that purification of our photoradiolabelled proteins by preparative size-exclusion small-molecule effectively removed all small-molecule contaminants since no uptake in the gall bladder or intestines was

observed in the PET images recorded with [^{89}Zr]ZrDFO-PEG$_3$-azepin-onartuzumab.

Biodistribution studies were performed at 72 h on all animals after the final imaging time point (Figure 5; supporting Figures S49–S51 and Table S2). *Ex vivo* analysis corroborated the PET data and confirmed the specific tumour uptake and low retention of [^{89}Zr]ZrDFO-PEG$_3$-azepin-onartuzumab in background tissues.

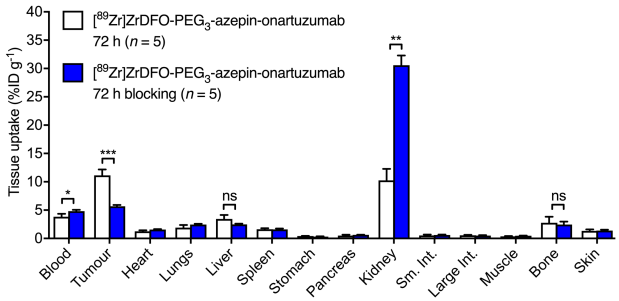

Figure 5. *Bar chart showing ex vivo biodistribution data (%ID g^{-1}) for the uptake of [^{89}Zr]ZrDFO-PEG$_3$-azepin-onartuzumab in the (normal group, white; blocking group, blue) in mice bearing MKN-45 tumours.*

Our experimental studies confirmed that photoradiosynthesis of ^{89}Zr-radiolabelled proteins with water-soluble DFO-derivatives produces viable PET radiotracers. However, proteins contain different nucleophiles that could attack the ketenimine intermediate produced by photoactivation of ArN_3 groups. To investigate the reaction coordinate for the light-induced activation of ArN_3 and to probe the potential reactivity of different nucleophiles, we used density functional theory (DFT; supporting Scheme S2, Table S3 and Figures S52–S55) calculations. intramolecular rearrangement and bimolecular reactions with AcO^- (modelling Glu / Asp residues) nucleophiles. Computational results indicated that nucleophilic attack by $MeNH_2$ (modelling Lys residues) at the ketenimine formed by photoactivation of compound **4** has a free energy barrier of +51.3 kJ mol^{-1}. In contrast, a significantly higher barrier of +62.8 kJ mol^{-1} was obtained with AcO^- as the incoming nucleophile (modelling Glu / Asp residues). Differences in the kinetic barriers (labelled as TS4 in Table S3) suggest that lysine residues are more likely to react than Glu/Asp carboxylate groups. Notably, extensive DFT studies were unable to find appropriate transition states for the attack of H_2O, HO^-, MeOH, MeO^-, MeSH, MeS^- nucleophiles at the ketenimine intermediates indicating that reactions with cysteine, threonine or serine residues are unlikely to occur by this mechanism. Further experiments are required to confirm the proposed chemoselectivity of light-induced protein-conjugation using photoactivatable ArN_3 compounds.

In conclusion, accessing water-soluble DFO-derivatives bearing discrete $(PEG)_3$ linkers is simple and facilitates the use of photochemistry in the synthesis of ^{89}Zr-mAbs. Further studies are underway to evaluate the impact of the PEG unit on the metabolic stability of protein-conjugates *in vivo*. Compound **4** has been produced in accordance with GLP regulations which will expedite the synthesis of clinical-grade ^{89}Zr-mAbs by photoradiosynthesis.

Experimental Section

Full experimental details and characterisation data are provided in the Supporting Information.

Acknowledgements

JPH thanks the Swiss National Science Foundation (SNSF Professorship PP00P2_163683 and PP00P2_190093), the Swiss Cancer League (Krebsliga Schweiz; KLS-4257-08-2017), and the University of Zurich (UZH) for financial support. This project has received funding from the European Union's Horizon 2020 research and innovation programme / from the European Research Council under the Grant Agreement No 676904, ERC-StG-2015, NanoSCAN. We thank all members of the Radiochemistry and Imaging Science group at UZH.

Keywords: Radiochemistry • photochemistry • positron emission tomography • antibody conjugates • zirconium-89

[1] O. Boutureira, G. J. L. Bernardes, *Chem. Rev.* **2015**, *115*, 2174–2195.

[2] J. P. Holland, M. Gut, S. Klingler, R. Fay, A. Guillou, *Chem. – A Eur. J.* **2019**, 1–18.

[3] N. P. Gritsan, M. S. Platz, *Chem. Rev.* **2006**, *106*, 3844–3867.

[4] M. S. Platz, *Acc. Chem. Res.* **1995**, *28*, 487–492.

[5] W. T. Borden, N. P. Gritsan, C. M. Hadad, W. L. Karney, C. R. Kemnitz, M. S. Platz, *Acc. Chem. Res.* **2000**, *33*, 765–771.

[6] M. Patra, L. S. Eichenberger, G. Fischer, J. P. Holland, *Angew. Chemie Int. Ed.* **2019**, *58*, 1928–1933.

[7] M. Patra, S. Klingler, L. S. Eichenberger, J. Holland, *iScience* **2019**, *13*, 416–431.

[8] L. S. Eichenberger, M. Patra, J. P. Holland, *Chem. Commun.* **2019**, *55*, 2257–2260.

[9] R. Fay, M. Gut, J. P. Holland, *Bioconjug. Chem.* **2019**, *30*, 1814–1820.

[10] M. Gut, J. P. Holland, *Inorg. Chem.* **2019**, *58*, 12302–12310.

[11] S. Klingler, R. Fay, J. P. Holland, S. Klingler, *J. Nucl. Med.* **2020**, in press.

[12] J. R. Dilworth, S. I. Pascu, *Chem. Soc. Rev.* **2018**, *47*, 2554–2571.

[13] G. Fischer, U. Seibold, R. Schirrmacher, B. Wängler, C. Wängler, *Molecules* **2013**, *18*, 6469–6490.

[14] T. Richardson-Sanchez, W. Tieu, M. P. Gotsbacher, T. J. Telfer, R. Codd, *Org. Biomol. Chem.* **2017**, *15*, 5719–5730.

[15] T. Richardson-Sanchez, R. Codd, *Chem. Commun.* **2018**, *54*, 9813–9816.

[16] M. Briand, M. L. Aulsebrook, T. L. Mindt, G. Gasser, *Dalton Trans.* **2017**, *46*, 16387–16389.

[17] J. P. Holland, *Inorg. Chem.* **2020**, *59*, 2070−2082.

[18] M. J. W. D. Vosjan, L. R. Perk, G. W. M. Visser, M. Budde, P. Jurek, G. E. Kiefer, G. A. M. S. van Dongen, *Nat. Protoc.* **2010**, *5*, 739–743.

[19] M. Merchant, X. Ma, H. R. Maun, Z. Zheng, J. Peng, M. Romero, A. Huang, N. -y. Yang, M. Nishimura, J. Greve, et al., *Proc. Natl. Acad. Sci.* **2013**, *110*, E2987–E2996.

10.1002/chem.202001755

WILEY-VCH

Entry for the Table of Contents

COMMUNICATION

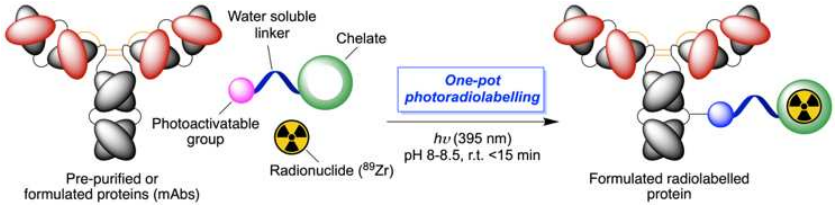

Photoradiosynthesis of ^{89}Zr-antibodies: Water-soluble, photoactivatable chelates derived from desferrioxamine B (DFO) have been synthesised and allow rapid, one-pot, protein-conjugation and ^{89}Zr-radiolabelling to produce antibody-based radiotracers for use in positron emission tomography (immuno-PET).

*Amaury Guillou, Daniel F. Earley and Jason P. Holland**

Page No. – Page No.

Light-activated protein-conjugation and ^{89}Zr-radiolabelling with water-soluble desferrioxamine derivatives